University College Dublin

School of Physics

Gamma - Frequency Resonance in Networks of Neurons

Literature Review

Author:
David Kelly

Supervisor:
Dr. Áine Byrne

Autumn Trimester 2024

Contents

1 Introduction to Mathematical Neuroscience

1.1 Historical Background

The study of the nervous system has evolved from early theories to the sophisticated neuroscience of today. Galen, an ancient Greek physician, believed the brain acted as a gland, transmitting fluid through nerves [18]. In the 19th century, Emil du Bois-Reymond and Hermann von Helmholtz demonstrated that nerves communicate electrically [4][2], and Golgi and Ramón y Cajal produced the first detailed neuron illustrations [19], foundational to modern neuroscience. Ross Granville Harrison's work on neuron growth [20] and Paul Ehrlich's discovery of receptor-based drug interactions [6] further advanced understanding.

Neuroscience has since diversified, with many different subdisciplines: molecular neuroscience studies neuron structures, systems neuroscience focuses on large neural networks, and cognitive neuroscience explores links between brain function and cognition. Mathematical approaches to studying the brain began in the 1940s with Norbert Wiener's cybernetics [17], which compared neural and computational processes, influencing von Neumann's work on digital computers [21].

A breakthrough in the 1950s by Hodgkin and Huxley introduced a quantitative model of action potentials, marking the start of mathematical neuroscience, which has since grown significantly [10]. Mathematical models of the brain can be either empirical, focusing on input-output relationships, or mechanistic, aiming to reflect structural details. Many models span multiple scales and strive for quantitative accuracy, revealing mechanisms underlying brain behavior and advancing interdisciplinary insights into neural functions [12].

1.2 Neurons

The neuron, as the foundational unit, serves as the starting point for studying this complex system. Neurons are specialized cells that transmit electrical signals, known as action potentials (APs), across distances, although at much slower speeds than light. Each neuron has essential parts: the soma (cell body), dendrites that receive incoming signals, and the axon, which transmits signals to other neurons, as seen in Figure 1.

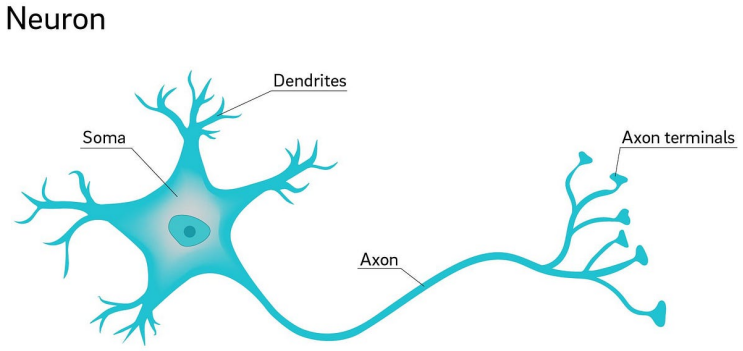

Figure 1: Neuron diagram [15].

Dendrites are tree-like extensions at the beginning of a neuron that help increase the surface area of the cell body. These tiny protrusions receive information from other neurons and transmit electrical stimulation to the soma. Dendrites are also covered with synapses. The soma, or cell body,

is where the signals from the dendrites are joined and passed on. The soma and the nucleus do not play an active role in the transmission of the neural signal. Instead, these two structures serve to maintain the cell and keep the neuron functional. The axon is the elongated fiber that extends from the cell body to the terminal endings and transmits the neural signal. The larger the diameter of the axon, the faster it transmits information. Some axons are covered with a fatty substance called myelin that acts as an insulator. These myelinated axons transmit information much faster than other/non-myelinated axons [5]. Axon terminals are the ends of axons that send messages to other cells by releasing chemicals called neurotransmitters at synapses [3].

There are two main types of neurons: projection neurons, which are often excitatory and carry signals long distances within the central nervous system (CNS) or brain regions, and interneurons, which have shorter axons and usually provide inhibitory inputs. An excitatory transmitter promotes the generation of an electrical signal called an action potential in the receiving neuron, while an inhibitory transmitter prevents it [8]. Projection neurons play a key role in the brain's cognitive functions, while interneurons modulate local circuits.

Dendrites receive inputs densely (about two per micrometer), with each neuron typically having a total of 4 mm of dendritic length. Neurons can form thousands of connections, and axons themselves have about 180 synapses per millimeter on average. Human neurons vary significantly in size and shape, with the longest axons reaching over a meter in length. In total, the human brain contains roughly 100 billion neurons, connected by about 100 trillion synapses, highlighting its immense complexity.

1.3 Action Potentials

The neuron's membrane contains numerous ion channels, which are specialized pores allowing selective passage of ions like sodium (Na^+), potassium (K^+), calcium (Ca^{2+}), and chlorine (Cl^-). These channels open or close in response to the membrane voltage (the electrical potential difference across the membrane) or external/internal signals. When the neuron is at rest, it maintains a resting potential of about -70 mV, kept stable by ion pumps that expel Na^+ ions and bring in K^+ ions. Ions move through channels according to concentration and voltage gradients, with positive ions moving toward lower potential areas and negative ions toward higher potential. Positive current, defined as outward ion flow, hyperpolarizes the cell (makes it more negative), while negative inward current depolarizes it (makes it more positive).

Depolarization can trigger a spike if it reaches a threshold level, causing a large voltage fluctuation known as an action potential (AP), which is the neuron's electrical output. During an action potential, the membrane voltage temporarily shifts by about 100 mV, rising from around -70 mV to a peak of approximately +30 mV. This spike begins as Na^+ channels open, allowing Na^+ ions to rush in and raise the membrane voltage, followed by the opening of K^+ channels that permit K^+ ions to flow out, restoring the voltage below resting levels as Na^+ channels close. After a spike, a neuron enters an absolute refractory period, where it cannot spike again, followed by a relative refractory period, during which spiking is not impossible but remains difficult as ion gradients recover.

Subthreshold potentials, or minor voltage changes that don't reach spike threshold, dissipate quickly along the axon and are undetectable beyond about 1 mm from the soma. Action potentials, in contrast, regenerate along the axon and travel without losing strength. This active wave propagation, facilitated by ionic movement across the membrane, differs from passive wave transmission, such as sound waves in air or electrical currents in wires. Certain cells, like retinal bipolar cells, exhibit only non-spiking, subthreshold voltage changes [12].

1.4 Synapses

Neurons communicate through two main types of connections: chemical synapses (synapses) and electrical synapses (gap junctions). Gap junctions allow direct electrical influence between neigh-

boring cells, functioning much like electrical resistors. At a chemical synapse, an axon from the presynaptic neuron contacts a dendrite on the postsynaptic neuron, as seen in Figure 2. When an action potential (AP) reaches the presynaptic terminal, Ca^{2+} channels open, allowing calcium to enter. This influx triggers neurotransmitter-filled vesicles to fuse with the membrane, releasing neurotransmitters into the synaptic cleft (space after axon terminal between the next target cell [13]). These neurotransmitters bind to receptors on the postsynaptic dendritic spine, opening ion channels that generate currents. These currents either excite (depolarize) or inhibit (hyperpolarize) the postsynaptic neuron, leading to excitatory or inhibitory postsynaptic potentials (EPSPs or IPSPs), respectively [12].

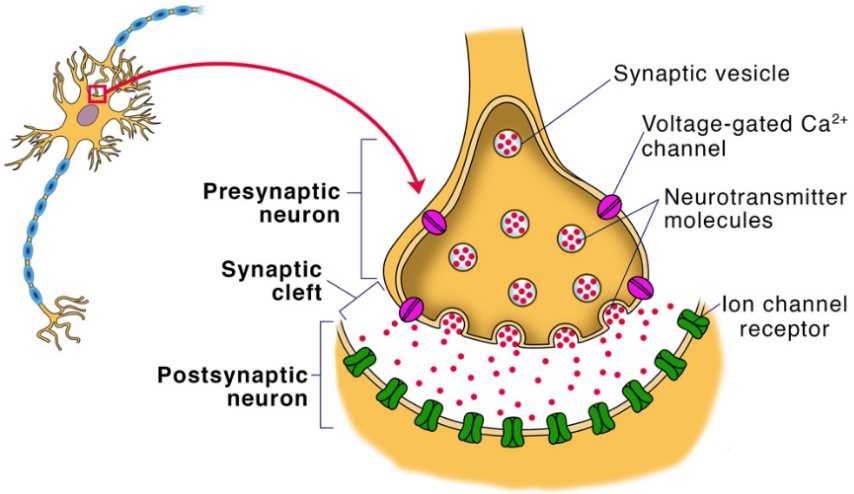

Figure 2: Synapse diagram [16].

2 Hodgkin - Huxley Model

The Hodgkin-Huxley model, developed by Alan Hodgkin and Andrew Huxley in the 1950s, is a foundational framework in neuroscience that explains how neurons generate action potentials. Based on experiments with the squid giant axon, the model describes the relationship between membrane potential and ionic currents, focusing on sodium (Na^+), potassium (K^+), and leak channels. Using a system of differential equations, it quantifies the dynamics of voltage-gated ion channels and their nonlinear interactions. This groundbreaking work earned Hodgkin and Huxley the Nobel Prize in Physiology or Medicine in 1963 and remains central to the study of neuronal excitability [1].

2.1 Ions

As mentioned above, neuronal electrical activity is sustained by ionic currents across the cell membrane, primarily involving sodium (Na^+), potassium (K^+), calcium (Ca^{2+}), and chloride (Cl^-) ions. Sodium, potassium, and calcium are positively charged cations, while chloride is a negatively charged anion. The different concentrations of these ions inside and outside the cell create electrochemical gradients that drive neural activity. The extracellular space is rich in Na^+, Cl^-, and Ca^{2+}, while the intracellular space has high K^+ concentrations and negatively charged molecules (A^-).

Ion channels in the cell membrane allow selective ion flow based on these electrochemical gradients, especially for K^+ and Cl^-. This movement maintains concentration differences due to two

factors:

Passive Redistribution: The impermeable intracellular anions (A^-) attract K^+ into the cell and repel Cl^-, maintaining the gradients.

Active Transport: Ion pumps, such as the Na^+ - K^+ pump, actively transport ions to uphold these gradients, moving three Na^+ ions out for every two K^+ ions brought in.

The Nernst potential describes the balance of forces driving ions across a cell membrane. Ion movement is influenced by both concentration and electrical potential gradients. For example, K^+ ions diffuse out of the cell because their concentration is higher inside than outside. As K^+ exits, it leaves behind a net negative charge, creating an outward current and an electric potential gradient across the membrane. This gradient slows K^+ diffusion as the positive ions are attracted back to the negative interior and repelled from the positive exterior. Eventually, an equilibrium is reached where the concentration and electric forces are balanced out, and net ion movement ceases.

The equilibrium potential for each ion is given by the Nernst equation [10]:

$$E_{\text{ion}} = \frac{RT}{zF} ln \frac{[\text{Ion}]_{\text{out}}}{[\text{Ion}]_{\text{in}}} \tag{2.1}$$

where:

- $[\text{Ion}]_{\text{in}}$ and $[\text{Ion}]_{\text{out}}$ are the ion concentrations inside and outside the cell.
- R is the gas constant.
- T is the temperature in Kelvin.
- F is Faraday's constant.
- z is the ion's valence (e.g., 1 for K^+ and Na^+, -1 for Cl^- and 2 for Ca^{2+}).

The ionic currents and conductances within neurons regulate membrane potentials and influence how signals are propagated. Membrane potential, V, is defined as the voltage difference across the cell membrane, and each ion has a corresponding Nernst potential (E_{Na}, E_{Ca}, E_{K} and E_{Cl}). When V equals a specific ion's equilibrium potential, its current (i.e., $I_{\text{Na/Ca/K/Cl}}$) is zero, creating no net ion movement. If V differs from an ion's equilibrium potential, the current becomes:

$$I_j = g_j(V - E_j), \quad \text{where } \ j \in [\text{Na}, \text{Ca}, \text{K}, \text{Cl}] \tag{2.2}$$

where g_j is the ion's conductance, acting as a driving force for ion flow.

Generally, ionic currents vary over time and are impacted by membrane voltage, neurotransmitters, and other agents, making them nonlinear. This variability enables neurons to produce action potentials, or spikes, as conductances change dynamically.

Neurons are often represented by an equivalent circuit model. Here, the total current I across the membrane consists of the membrane capacitive current and the sum of ionic currents:

$$I = C\frac{dV}{dt} + I_{\text{Na}} + I_{\text{Ca}} + I_{\text{K}} + I_{\text{Cl}} \tag{2.3}$$

If no external current flows into the cell, $I = 0$, and the resting membrane potential V_{rest} balances inward (e.g., I_{Na}, I_{Ca}) and outwards (e.g., I_{K}, I_{Cl}) currents, given by:

$$V_{\text{rest}} = \frac{g_{\text{Na}}E_{\text{Na}} + g_{\text{Ca}}E_{\text{Ca}} + g_{\text{K}}E_{\text{K}} + g_{\text{Cl}}E_{\text{Cl}}}{g_{\text{Na}} + g_{\text{Ca}} + g_{\text{K}} + g_{\text{Cl}}} \tag{2.4}$$

The term $g_{\text{inp}} = g_{\text{Na}} + g_{\text{Ca}} + g_{\text{K}} + g_{\text{Cl}}$ represents the total input conductance, with its reciprocal $R_{\text{inp}} = 1/g_{\text{inp}}$ defining the membrane's input resistance, which modulates the voltage response to injected currents.

At rest, potassium and chloride conductances dominate, keeping V near their equilibrium potentials. When an action potential occurs, however, sodium or calcium conductances briefly increase, driving V closer to their respective equilibrium values. This mechanism underlies the rapid voltage changes central to neural signaling [10].

Despite the stochastic nature of individual channel gating, the collective behaviour of a large population of identical channels can be captured by the equation:

$$I = \bar{g}p(V - E) \tag{2.5}$$

where:

- I is the net ionic current.
- $\bar{g}$ is the maximal conductance of the population.
- p is the average proportion of channels in the open state.
- E is the reversal potential for the current (equivalent to the Nernst equilibrium potential for selective channels).

2.1.1 Voltage - Gated Channels

Voltage-gated channels have gates sensitive to membrane potential, which can activate (open) or inactivate (close) the channel. The activation probability for Na^+ channels is denoted by m, while h represents the probability of inactivation. The proportion of open channels p can be expressed as:

$$p = m^a h^b \tag{2.6}$$

Here, a is the number of activation gates and b is the number of inactivation gates per channel. Channels can be partially activated ($0 < m < 1$), completely open ($m = 1$), or closed ($m = 0$). Inactivated channels have $h = 0$, while those released from inactivation have $h = 1$. Channels without activation gates result in persistent currents, while those with inactivation produce transient currents.

2.1.2 Dynamics of Activation and Inactivation

Both the activation variable m and the inactivation variable h of voltage - gated ion channels are governed by similar first - order differential equations:

$$\dot{y} = \frac{(y_\infty(V) - y)}{\tau(V)} \tag{2.7}$$

where y represents either m or h. In this equation:

- $y_\infty(V)$ is the steady - state function:
  - For activation, $m_\infty(V)$ indicates the maximum value of m at a fixed membrane potential V. It typically exhibits a sigmoid shape.
  - For inactivation, $h_\infty(V)$ describes the proportion of inactivation gates open at a given V.
- $\tau(V)$ is the time constant, determining how quickly y reaches its steady - state value. It generally has a unimodal shape.

Voltage - clamp experiments help characterize $h_\infty(V)$ by initially holding the membrane at a pre-step potential until the activation and inactivation variables reach steady states, followed by a step increase in voltage. This approach allows researchers to determine how inactivation depends on prior membrane potential conditions.

2.2 Hodgkin - Huxley Equations

The Hodgkin - Huxley model quantifies the nonlinear interactions between membrane potential and ionic currents, and it is based on three main currents:

- **Voltage - Gated Persistent K^+ Current:** Described by an activation variable n, this current depends on four activation gates, resulting in a term n^4 in the model's equations.
- **Voltage - Gated Transient Na^+ Current:** This current has three activation gates and one inactivation gate, modeled as m^3h.
- **Leak Current (I_L):** This is an Ohmic current carried primarily by chloride ions (Cl^-).

The space-clamped Hodgkin-Huxley equations assume a uniform membrane potential, eliminating spatial variations to focus on ionic currents and voltage - dependent conductances:

$$C\frac{dV}{dt} = I - \bar{g}_{\mathrm{K}}n^4(V - E_{\mathrm{K}}) - \bar{g}_{\mathrm{Na}}m^3h(V - E_{\mathrm{Na}}) - g_{\mathrm{L}}(V - E_{\mathrm{L}}) \tag{2.8}$$

where:

- C is the membrane capacitance.
- $\bar{g}_{\mathrm{K}}$, $\bar{g}_{\mathrm{Na}}$ and g_{L} are the maximal conductances for K^+, Na^+ and leak currents, respectively.
- E_{K}, E_{Na} and E_{L} are the reversal potentials for each ion type.

The dynamic variables n, m and h represent probabilities related to the gating of K^+ and Na^+ channels and are described by differential equations of the form:

$$\frac{dc}{dt} = \alpha_c(V)(1 - c) - \beta_c(V)c, \quad \text{where } c \in [n, m, h] \tag{2.9}$$

Here α and β are voltage - dependent rate functions for the transitions between open and closed states of each gate.

The equilibrium potentials are; $E_{\mathrm{K}} = 53\mathrm{mV}$, $E_{\mathrm{Na}} = 185\mathrm{mV}$, $E_{\mathrm{L}} = 75.6\mathrm{mV}$. Typical values for maximal conductances are; $\bar{g_{\mathrm{K}}} = 36\ \mathrm{mS/cm^2}$, $\bar{g_{\mathrm{Na}}} = 120\ \mathrm{mS/cm^2}$, $g_{\mathrm{L}} = 0.3\ \mathrm{mS/cm^2}$.

To simplify, the original Hodgkin-Huxley equations can also be written using steady-state activation/inactivation functions and time constants:

$$\frac{dc}{dt} = \frac{c_\infty(V) - c}{\tau_c(V)}, \quad c \in [n, m, h] \tag{2.10}$$

where:

$$c_\infty(V) = \frac{\alpha_c(V)}{\alpha_c(V) + \beta_c(V)}, \quad \tau_c(V) = \frac{1}{\alpha_c(V) + \beta_c(V)}, \quad c \in [n, m, h] \tag{2.11}$$

These reformulated equations are advantageous because they separate steady-state behavior and dynamic response times, providing a clearer picture of how each variable approaches equilibrium.

While the Hodgkin-Huxley model was derived for the squid giant axon, it provides a generalizable framework for describing ion channel kinetics in many types of neurons. In the central nervous system, neurons may have additional currents, each with unique activation and inactivation kinetics that can be incorporated using this formalism.

In conclusion, the Hodgkin-Huxley equations effectively model the action potential's genesis and provide a rich basis for understanding the nonlinear interactions between membrane potential and ionic currents. This model remains fundamental in computational neuroscience, where it supports more complex studies of neuronal dynamics and excitability.

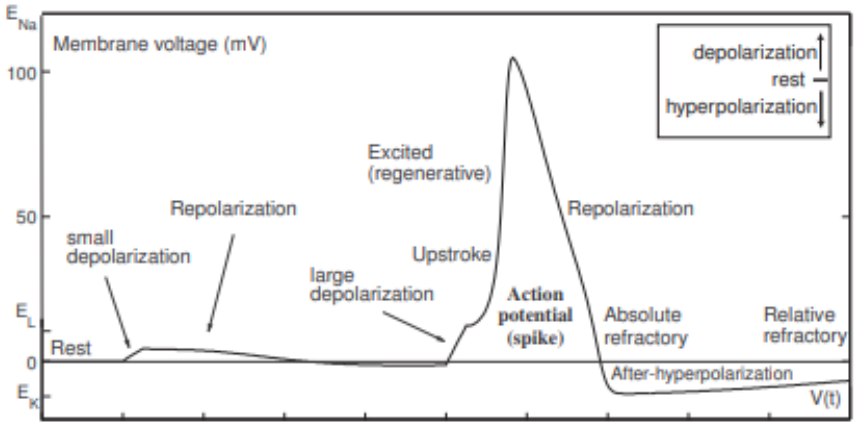

Figure 3: Action Potential in the Hodgkin - Huxley Model [10].

3 Simple Models

3.1 Integrate - and - Fire

The integrate - and - fire model simplfies neuronal dynamics by representing subthreshold behaviour with Ohmic leakage. This behaviour is captured by the differential equation:

$$C\frac{dV}{dt} = I - g_{\text{leak}(V-E_{\text{leak}})} \tag{3.1}$$

where C is the membrane capacitance, g_{leak} is the leakage conductance and E_{leak} is the leakage potential. When the membrane potential V reaches a threshold E_{thresh}, the neuron is said to 'fire' and V is reset to E_K.

In its rescaled form, the model can be represented as:

$$\frac{dv}{dt} = b - v, \quad \text{if } v = 1, \text{ then } v \leftarrow 0 \tag{3.2}$$

where v is the normalized voltage, b represents resting state, and $v = 1$ is the threshold. This model fires periodically when $b > 1$ with period $T = -\ln(1 - 1/b)$. Some of the key features of this model are as follows:

- **All - or - none spiking:** Spikes are uniform in size and duration.
- **Threshold and Refractory Period:** Clear spike threshold with a brief period of deceased excitability post - spike.
- **Class 1 Excitability:** Modulates firing rate based on input intensity.

While computationally efficient, the integrate - and - fire model lacks realistic bifurcation dynamics and spike latency, making it suitable primarily for theoretical studies rather than detailed spiking simulations.

3.2 Resonate - and - Fire

The resonant - and - fire model extends the integrate - and - fire by introducing resonant currents, adding a second variable W to denote the magnitude of such currents. This is described by:

$$C\frac{dV}{dt} = I - g_{\text{leak}}(V - E_{leak}) - W \tag{3.3}$$

$$\frac{dW}{dt} = \frac{V - V_{1/2}}{k} - W \tag{3.4}$$

If $V \geq V_{\text{thresh}}$, the neuron "fires", resetting V and W to specified values. This model can be further simplified with complex coordinates as:

$$\frac{dz}{dt} = (b + iw)z + I \tag{3.5}$$

where $z = x+iy$. The real part, x, is a current-like variable. It describes the dynamics of the resonant current and synaptic currents. The imaginary part, y, is a voltage-like variable. The neuron is said to fire a spike when y reaches the threshold y = 1 [10]. When the spike fires, z is reset to z_{reset}. Some of the key features of this model are:

- **Damped Oscillations and Rebound Spiking:** Exhibits frequency preference and post - inhibitory spiking.
- **Excitability:** Fires periodically without a directly proportional frequency response to input.

The resonant - and - fire model effectively captures resonant neuron behavior but, like the integrate - and - fire model, does not represent detailed spike waveforms, making it more suitable for mathematical analysis than for detailed neuronal simulations.

4 Izhikevich Neuron Model

The Izhikevich model is a simplified two-dimensional model that captures a neuron's subthreshold dynamics by using two main variables: a fast voltage variable and a slower recovery variable. The recovery variable generally represents the activity of potassium channels, the inactivation of sodium channels, or a combination of these. Like integrate-and-fire models, the Izhikevich model emphasizes efficiency in simulation over intricate details of spike generation [7].

In this model, the voltage is allowed to increase towards a defined peak. When this peak is reached, the recovery variable receives a positive current, and the voltage resets to the resting level. Mathematically, the model is represented as:

$$\frac{dv}{dt} = 0.04v^2 + 5v + 140 - u + I \tag{4.1}$$

$$\frac{du}{dt} = a(bv - u) \tag{4.2}$$

with a post-spike reset condition:

$$\text{if } v \geq 30\text{mV}, \text{ then } \begin{cases} v \leftarrow c \\ u \leftarrow u + d \end{cases} \tag{4.3}$$

In this framework, v and u are dimensionless variables and a, b, c and d are dimensionless parameters. The variable v, denotes the neuron's membrane potential, while u is the recovery variable that models the activation of potassium (K^+) currents and the inactivation of sodium (Na^+) currents, providing negative feedback to v. After each spike its peak value (+30mV), the volatge v and recovery variable u are reset as specified in the condition. Synaptic currents or externally applied DC currents are incorporated through variable I [9].

In the model used in this project, a noise term and synaptic connectivity term was added. The noise term $J_j(t)$ is represented by a random process with zero mean and variance σ_N. The k_j term is just a scaling factor. The parameters for the synaptic connectivity term are E_{syn} for the synaptic reversal potential, g_{ij} for the synaptic conductance and s_{ij} for the synaptic activation levels. The i

and j index subscripts just denote the ith and jth neuron in the population. Note that autosynapses are prohibited; that is, $g_{ij} = 0$ if $i = j$ [14].

$$\frac{dv_j}{dt} = k_j(0.04v_j^2 + 5v_j + 140 - u_j + I_j) + J_j(t) - (v_j - E_{\text{syn}}) \sum_{i=1}^{N} g_{ij} s_{ij}(t) \tag{4.4}$$

$$\frac{du_j}{dt} = k_j a(bv_j - u_j) \tag{4.5}$$

The second order synaptic coupling is used to describe s_{ij}, and is given as,

$$\left(1 + \tau_s \frac{d}{dt}\right)^2 s = -\frac{1}{N} \sum_q \sum_j \delta(t - t_j^q) \tag{4.6}$$

which can be written as two first order differential equations,

$$\begin{cases} \frac{ds}{dt} = -\frac{s}{\tau_s} + \frac{p}{\tau_s} \\ \frac{dp}{dt} = -\frac{p}{\tau_s} + \frac{1}{\tau_s} \sum^{K_{ij}} \sum \left(\delta(t - t_j^q)\right) \end{cases} \tag{4.7}$$

$$\text{if } \; v_j \geq 30\text{mV}, \;\; \text{then } \begin{cases} v_j \to c \\ u_j \to u_j + d \\ p \to \frac{1}{\tau_s} \end{cases} \tag{4.8}$$

Here, s_{ij} represents the synaptic state or coupling strength between neurons i and j, capturing capturing the dynamics of synaptic activation resulting from presynaptic spikes. The term τ_s is the synaptic time constant, which governs the rate of decay for the synaptic state and is chosen such that the peak synaptic activation normalizes to 1. The Dirac delta function $\delta(t - t_j^q)$ accounts for accounts for discrete spike events, contributing to the dynamics of s and p whenever a presynaptic neuron j spikes at time t_j^q. The auxiliary variable p simplifies the second-order dynamics into two coupled first-order equations, representing intermediate processes that influence s.

The double summation $\sum^{K_{ij}} \sum \left(\delta(t - t_j^q)\right)$ accounts for the spikes from all presynaptic neurons connected to neuron i through the synaptic network K_{ij}, while the normalization factor $\frac{1}{N}$ scales these contributions by the number of inputs. The spike condition $v_j \geq 30$mV, reflects the firing threshold of neuron j, after which the membrane potential v_j resets to a value c, the recovery variable u_j is incremented by d, and p is updated to reflect the synaptic contribution of the spike. When a neuron spikes, $\frac{dp}{dt}$ temporarily equals $-\frac{p}{\tau_s}$, ensuring that p begins decaying exponentially following the spike event [22].

4.1 Synchrony Measures

In mathematical neuroscience, synchrony measures provide quantitative ways to assess how neurons or neural populations interact and align over time. These metrics are crucial in understanding network dynamics, such as how groups of neurons coordinate to encode information, respond to stimuli, or potentially lead to pathological conditions (e.g., seizures). Synchrony measures help describe both the overall behavior of neural networks and the variability or stability in their responses, providing insights into neural coding, reliability, and the effects of external inputs on neural dynamics.

4.1.1 χ^2 Measurement

The χ^2 measure quantifies synchrony among neurons by comparing the variance of the network's average voltage to the average of the individual neurons' voltage variances. Specifically, it is defined as:

$$\chi^2(N) = \frac{\sigma_V^2}{\frac{1}{N}\sum_N^{i=1}\sigma_{Vi}^2} \tag{4.9}$$

where N is the number of neurons, σ_V^2 is the variance of the mean voltage across neurons, and $\sigma_{V_i}^2$ is the variance of each neuron's voltage individually. This measure has a range from 0 to 1. $\chi^2 = 1$ indicates perfect synchrony, where all neurons have identical voltage variance over time resulting in fully synchronized activity. $\chi^2 = 0$ occurs when neurons are completely asynchronous, as the variance of the mean voltage across neurons approaches zero [7].

4.1.2 Reliability Measurement

Hunter et al. [11] introduced a reliability measure to assess the synchrony of neuron spike timing in their study on the resonance effect for spike time reliability. The measure, R, is defined as the variance of the summed, convolved spike trains of each neuron:

$$R = \int X^2(t)dt - \left(\int X(t)dt\right)^2 \tag{4.10}$$

where $X(t)$ represents the sum of the spike trains of all neurons, convolved with a kernel $h(t)$. The kernel is defined as:

$$h(t) = \frac{1}{\tau_R}e^{-\frac{t}{\tau_R}} \tag{4.11}$$

and τ_R is chosen based on the firing frequency of the neurons. Specifically τ_R is selected so that the effect of a spike decays before the next spike from the same neuron, ensuring temporal independence within the kernel application. This choice ensures consistency in measuring synchrony and aligns with the Van Rossum distance metric, which uses the same kernel to quantify spike train similarity.

When neurons fire in synchrony, the sum $X(t)$ has narrow, tall spikes, resulting in high variance in R, which implies high reliability. When neurons are asynchronous, $X(t)$ becomes approximately constant, leading to low variance and therefore a low reliability.

To ensure that R lies between 0 and 1, a maximum theoretical value $R_{\max}$ is derived based on neuron and spike parameters:

$$R_{\max} = \frac{N^2M}{2T\tau_R} - \frac{N^2M^2}{T^2} \tag{4.12}$$

where N is the number of neurons, M is the total number of spikes and T is the total simulation time.

By scaling R by $R_{\max}$, the reliability measure achieves a maximum of 1 for complete synchrony (high variance) and a minimum of 0 for complete asynchrony (low variance). This scaling normalizes the reliability measure, allowing it to represent synchrony as a value between 0 and 1 [7].

5 Implementation of the Izhikevich Model

5.1 Determining τ_s

Tikidji-Hamburyan et al. [14] use a different set of equations to determine s_{ij};

$$s_{ij} = \beta_j - \alpha_j; \quad \frac{d\alpha_j}{dt} = -\frac{\alpha_j}{\tau_{\text{rise}}}; \quad \frac{d\beta_j}{dt} = -\frac{\beta_j}{\tau_{fall}} \tag{5.1}$$

where α_j and β_j represent the rise and fall dynamics of the synaptic response, governed by their respective time constants τ_{rise} and τ_{fall}. The second - order synaptic coupling employs a different approach characterized by equation (4.6). Since the s_{ij} is different, a comparison is necessary to tune the τ_s parameter in the second - order model. Specifically, the goal is twofold:

1. To ensure that the spike timing in the second - order model aligns with the expected dynamics of the s_{ij} variable described in the paper.

2. To ensure that the peak value of s_{ij} reaches 1, which is critical for consistency with the theoretical framework and empirical observations in the paper.

To achieve these objectives, the dynamics of s_{ij} in both models were compared by solving their respective differential equations numerically. For the model used in [14], α_j and β_j, were computed using their time constants, τ_{rise} and τ_{fall} given as 2ms and 5ms respectively. The second - order model was governed by the parameter τ_s, which controls the temporal evolution of $s(t)$.

The comparison focused on aligning spike timing and ensuring the peak amplitude of $s(t)$ reached 1. By systematically adjusting τ_s, the second - order model was tuned to replicate the dynamics of s_{ij} from the model used in [14]. Figure 4 illustrates the results, with spike timing marked by a red vertical line and the peak value of $s(t) = 1$ indicated by a black horizontal line. This validation confirms that τ_s can effectively align the second - order model with the observation in [14].

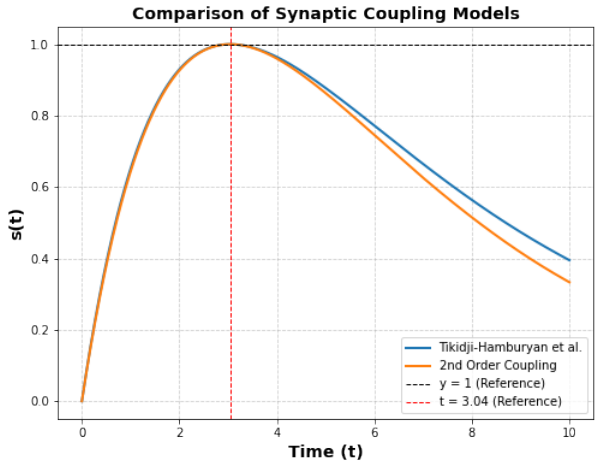

Figure 4: Comparing the synaptic coupling models of Tikidji-Hamburyan et al. [14] and second-order coupling.

5.2 Simulation Parameters and Model Setup

Network Configuration

The network consisted of $N = 300$ neurons simulated over a duration of $T = 300$ms with a time step $\Delta t = 0.005$ms. The network employed sparse, probabilistic connectivity, with an average of 40 connections per neuron. Connections were determined by a probability of $P = 0.133$ (= Average Connections/N), and the synaptic coupling strength for each connection was fixed at $g = 0.03$.

For all - to - all connectivity, every neuron was connected to all other neurons in the network, ensuring a fully connected structure. To maintain consistency with the sparse connectivity setup, the synaptic coupling strength (g) for all - to - all connectivity was set as the average value of the coupling matrix from the sparse connectivity case. This ensured that the total synaptic input to each neuron remained comparable across both connectivity schemes, allowing for meaningful comparisons of network dynamics.

Neuron Model Parameters

The neurons were modeled with parameters chosen to reflect realistic spiking dynamics:

- Voltage Dynamics: The membrane potential (v) evolved according to a quadratic equation with a reset threshold of 30mV and a reset value of -65mV after spiking. Synaptic inputs were modeled as inhibitory, with a reversal potential of $E_{\text{syn}} = -70$mV, influencing the postsynaptic potential through the synaptic coupling term.
- Recovery Variable: The recovery variable (u) captured the slow recovery dynamics after spiking, governed by $a = 0.1$ (recovery rate) and $b = 0.26$ (sensitivity to membrane potential changes). After spiking, u was incremented by $d = -1$.
- A constant input current of $I = 0.15$ was applied to all neurons. Additionally, a random background currents (J) were drawn from a normal distribution with a mean of 0 and a standard deviation of 0.25.

Synaptic Coupling

Synaptic connections were modeled as inhibitory, with a reversal potential of $E_{\text{syn}} = -70$mV. The dynamics of synaptic activity were governed by a second-order coupling term, characterized by a time constant $\tau_s = 3.043$ms. The synaptic state variables s and p evolved dynamically, contributing to the membrane potential of connected neurons.

Initial Conditions

To reflect variability in neuronal states, the initial membrane potentials (v_{init}) were drawn from a normal distribution with a mean of -70mV and a standard deviation of 5. Recovery variables (u_{init}) and synaptic state variables ($s_{\text{init}}, p_{\text{init}}$) were initialized to 0.

Spike Detection and Numerical Integration

Spike detection was implemented by identifying when a neuron's membrane potential exceeded 30mV. Following a spike, the membrane potential was reset, and synaptic variables were updated accordingly. The equations were integrated using a high-precision numerical solver with a relative tolerance of 10^{-8}.

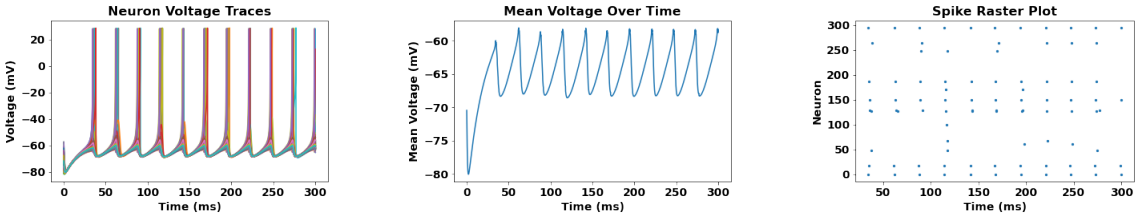

(a) Neuron Voltage Traces (b) Mean Voltage (c) Spike Raster Plot

Figure 5: The three plots illustrate the network dynamics: (a) neuron voltage traces, (b) mean voltage over time, and (c) spike raster plot for sparsely connected networks.

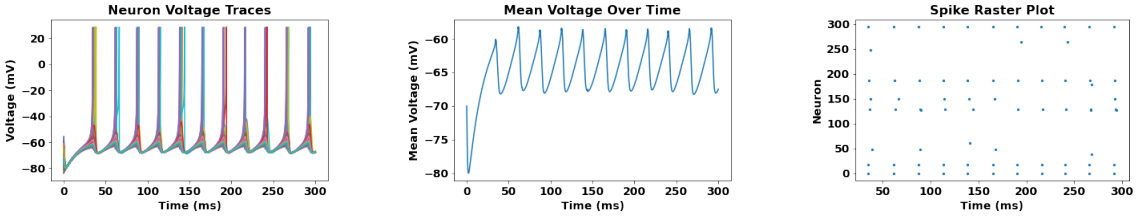

(a) Neuron Voltage Traces (b) Mean Voltage (c) Spike Raster Plot

Figure 6: The three plots illustrate the network dynamics: (a) neuron voltage traces, (b) mean voltage over time, and (c) spike raster plot for all - to - all connected networks.

The χ^2 value for the sparsely connected network shown in Figure 5 was determined to be 0.616 and 0.642 for all - to - all connected networks. Since the average value of the coupling matrix for the sparsely connected network was used as the connection strength for the all - to - all connected system, these χ^2 values are very similar indicating the relation between the connection probability (number of interconnected neurons) and the coupling strength.

6 Appendix

6.1 Hodgkin - Huxley Equations

The α and β functions mentioned in equations 2.9 - 2.11 are voltage - dependent rate functions for the transitions between open and closed states of each gate. These rate functions are:

$$\alpha_n(V) = 0.01\frac{10-V}{\exp\left(\frac{10-V}{10}\right)-1}, \quad \beta_n(V) = 0.125\exp\left(\frac{-V}{80}\right) \tag{6.1}$$

$$\alpha_m(V) = 0.1\frac{25-V}{\exp\left(\frac{25-V}{10}\right)-1}, \quad \beta_m(V) = 4\exp\left(\frac{-V}{18}\right) \tag{6.2}$$

$$\alpha_h(V) = 0.07\exp\left(\frac{-V}{20}\right), \quad \beta_h(V) = \frac{1}{\exp\left(\frac{30-V}{10}\right)+1} \tag{6.3}$$

References

[1] A.F. Huxley A.L. Hodgkin. A quantitative description of membrane current and its application to conduction and excitation in nerve. *The Journal of Physiology*, 1952.

[2] Robert W. Baloh. Electricity and the nervous system. https://link.springer.com/chapter/10.1007/978-3-031-62994-5_5?, August 2024.

[3] Keta Bhaktal. Axon function, meaning and types, what is an axon? - video and lesson transcript. https://study.com/learn/lesson/what-is-an-axon-terminal-function-types.html?srsltid=AfmBOorDK1aF12KB0zEa3AWQGFeKKnoSzjWelCfRlQmjZYv_WlHuk2ML, November 2024.

[4] Encyclopedia Britannica. Emil heinrich du bois-reymond. https://www.britannica.com/biography/Emil-Heinrich-Du-Bois-Reymond, November 2024.

[5] Kendra Cherry. An overview of the different parts of a neuron. https://www.verywellmind.com/structure-of-a-neuron-2794896, November 2024.

[6] Laia Rosich Fèlix Bosch. The contributions of paul ehrlich to pharmacology: A tribute on the occasion of the centenary of his nobel prize. *Pharmacology*, 2008.

[7] Pablo Vizcaíno García. Validating the use of simplified models for studying gap junction coupling in the brain. Master's thesis, UCD School of Physics, 2023.

[8] Queensland Brain Institute. What are neurotransmitters? https://qbi.uq.edu.au/brain/brain-anatomy/what-neuron, November 2024.

[9] Eugene M. Izhikevich. Simple model of spiking neurons. *IEEE Transactions on Neural Networks*, 2003.

[10] Eugene M. Izhikevich. *Dynamical Systems in Neuroscience, The Geometry of Excitability and Bursting*. The MIT Press, 2007.

[11] P.J. Thomas J.D. Cowan J.D. Hunter, J.G. Milton. Resonant effect for neural spike time reliability. *Journal of Neurophysiology*, 1998.

[12] Kolia Sadeghi Michael Schwemmer Philip Eckhoff, Philip Holmes and KongFatt Wong-Lin. *A Short Course in Mathematical Course*. Princeton University, 2015.

[13] Amanda Robb. Synaptic cleft - definition, function and activity. https://study.com/academy/lesson/synaptic-cleft-definition-function.html, November 2024.

[14] John A. White Ruben A. Tikidji-Hamburyan, Joan José Martínez and Carmen C. Canavier. Resonant interneurons can increase robustness of gamma oscillations. *The Journal of Neuroscience*, 2015.

[15] Jain Sanskar. Mp neurons. https://medium.com/@sanskarjain15039/mp-neurons-c2fc2c177cf0, November 2024.

[16] ScienceFacts.net. What is a synapse? https://www.sciencefacts.net/synapse.htm, November 2024.

[17] Norbert Wiener. *Cybernetics: Or Control and Communication in the Animal and the Machine*. The M.I.T. Press, 1948.

[18] Wikipedia. Galen. https://en.wikipedia.org/wiki/Galen, November 2024.

[19] Wikipedia. History of neuroscience. https://en.wikipedia.org/wiki/History_of_neuroscience, November 2024.

[20] Wikipedia. Ross granville harrison. https://en.wikipedia.org/wiki/Ross_Granville_Harrison, November 2024.

[21] Wikipedia. von neumann architecture. https://en.wikipedia.org/wiki/Von_Neumann_architecture, November 2024.

[22] Richard Naud Wulfram Gerstner, Werner M. Kistler and Liam Paninski. *Neuronal Dynamics: From Single Neurons to Networks and Models of Cognition*. Cambridge University Press, 2014.